DEUTSCHES ELEKTRONEN-SYNCHROTRON DESY

DESY 80/49
June 1980

CHARGED PION, KAON, PROTON AND ANTI-PROTON PRODUCTION IN HIGH ENERGY e^+e^- ANNIHILATION

TASSO Collaboration

NOTKESTRASSE 85 · 2 HAMBURG 52

DESY 80/49
June 1980

Charged Pion, Kaon, Proton and Anti-Proton Production in High Energy e^+e^- Annihilation

TASSO Collaboration

R.Brandelik, W.Braunschweig, K.Gather, V.Kadansky, K.Lübelsmeyer, P.Mättig, H.-U.Martyn, G.Peise, J.Rimkus, H.G.Sander, D.Schmitz, A.Schultz von Dratzig, D.Trines, W.Wallraff,
I.Physikalisches Institut der RWTH Aachen, Germany[£]

H.Boerner, H.M.Fischer, H.Hartmann, E.Hilger, W.Hillen, L. Koepke, H. Kolanoski, G. Knop, P. Leu, B.Löhr[†], R.Wedemeyer, N.Wermes, M.Wollstadt,
Physikalisches Institut der Universität Bonn, Germany[£]

H.Burkhardt, D.G.Cassel[*], D.Heyland, H.Hultschig, P.Joos, W.Koch, P.Koehler[**], U.Kötz, H.Kowalski, A.Ladage, D.Lüke, H.L.Lynch, G.Mikenberg[***], D.Notz, J.Pyrlik, R.Riethmüller, M.Schliwa[††], P.Söding, B.H.Wiik, G.Wolf,
Deutsches Elektronen-Synchrotron DESY, Hamburg, Germany

R.Fohrmann, M.Holder, G.Poelz, O.Römer, R.Rüsch, P.Schmüser,
II. Institut für Experimentalphysik der Universität Hamburg, Germany[£]

D.M.Binnie, P.J.Dornan, N.A.Downie, D.A.Garbutt, W.G.Jones, S.L.Lloyd, D.Pandoulas, J.Sedgbeer, S.Yarker, C.Youngman,
Department of Physics, Imperial College London, England[££]

R.J.Barlow, I.Brock, R.J.Cashmore, R.Devenish, P.Grossmann, J.Illingworth, M.Ogg, B.Roe[****], G.L.Salmon, T.Wyatt,
Department of Nuclear Physics, Oxford University, England[££]

K.W.Bell, B.Foster, J.C.Hart, J.Proudfoot, D.R.Quarrie, D.H.Saxon, P.L. Woodworth,
Rutherford Laboratory, Chilton, England[££]

Y.Eisenberg, U.Karshon, D.Revel, E.Ronat, A.Shapira,
Weizmann Institute, Rehovot, Israel[£££]

J.Freeman, P.Lecomte, T.Meyer, Sau Lan Wu, G.Zobernig,
Department of Physics, University of Wisconsin, Madison, Wisconsin, USA[££££]

---

* On leave from Cornell University, Ithaca, NY, USA
** On leave from FNAL, Batavia, IL, USA
*** On leave from Weizmann Institute, Rehovot, Israel
**** On leave from the University of Michigan, Ann Arbor, MI, USA

† Now at SLAC, Stanford, CA, USA
†† Now at mbp Bremen, Germany

£ Supported by the Deutsches Bundesministerium für Forschung und Technologie
££ Supported by the UK Science Research Council
£££ Supported by the Minerva Gesellschaft für die Forschung mbH, München
££££ Supported in part by the US Department of Energy contract WY-76-C-02-0881.

Abstract

Production of pions, kaons, protons and anti-protons has been studied in e^+e^- annihilations at 12 and 30 GeV centre of mass energy using time of flight techniques. The fractional yield of charged kaons and baryons appears to rise with outgoing particle momentum. At our highest energy at least 40 % of e^+e^- annihilations into hadrons are estimated to contain baryons.

The multiplicity of charged particles in e^+e^- annihilation has been observed to grow rapidly[1,2,3] with rising centre of mass energy, the increase being concentrated in the small x_p region ($x_p = 2p/W$ where p is particle momentum and W the centre of mass energy). In this letter we present first measurements of the separation of the charged particle yield in the small x_p region into pions, kaons and nucleons for W = 12 GeV and for W between 27 and 31.6 GeV (called 30 GeV below). The measurements were performed at PETRA using the TASSO detector. Particle identification was made by means of a time of flight (TOF) measurement between the beam crossing signal and two groups of scintillation counters. The central part of the TASSO detector has been described previously[4] as have the trigger and cuts used in this experiment to select e^+e^- annihilations into hadrons[5].

Between the central tracking chambers and the coil and at a radial distance from the beamline of 132 cm are the 48 Inner Time of Flight (ITOF) counters covering 82 % of the solid angle. An rms resolution (σ) of 0.45 nsec has been achieved which includes jitter from the beam crossing signal. We use the ITOF counters to provide π-K separation up to a momentum of 0.6 GeV/c and (π/K)-p separation up to 1 GeV/c. We do not consider timing information from ITOF counters into which two or more charged tracks have penetrated.

Fig. 1(a) shows the reconstructed mass squared from ITOF information for tracks with momentum (0.4 - 0.6) GeV/c for the 30 GeV data. We calculate for each track particle hypothesis weights W_i ($i = \pi, K, p$) where $W_i = e^{-(\tau_m - \tau_i)^2/2\sigma^2}$, τ_m is the measured flight time and τ_i is the expected flight time for hypothesis i. We define pions and kaons by the weight W_π or W_K being more than three times any other W_i. Ambiguous (π-K) tracks, which occur at high momentum, are responsible for uncertainties of approximately 3 (30) % in the $\pi^\pm(K^\pm)$ signal in the momentum range (0.5 - 0.6) GeV/c. Ambiguous (π-K) tracks are classified as pions. We define protons and antiprotons by the simple cut of $0.6 < m^2 < 1.2$ GeV^2 (where m^2 is the reconstructed mass squared) for momenta less than 1 GeV/c. The $p,\bar{p}$ signal for the 30 GeV data is shown in the insert to Fig. 1(a).

In order to compute cross sections for π, K and $p,\bar{p}$ from the ITOF data several corrections have to be applied. The major track loss for $K^\pm$ comes from particle decay in flight and is typically 25 % at 0.5 GeV/c. In addition there are losses from interactions in the beam pipe which, for momenta greater than 0.3 GeV/c, are estimated to be ~5 % for $\pi^\pm$, $K^\pm$ and p but ~15 % for $\bar{p}$. We limit our $K^\pm$ measurements to (0.4 - 0.6) GeV/c and our $p,\bar{p}$ measurements to (0.5 - 1.0) GeV/c owing to energy loss in the beam pipe at lower momenta. A background of 15 ± 5 % is estimated to be present in the ITOF pion sample coming from misidentified electrons. The background from muons is negligible. In addition a small background is present in our $p,\bar{p}$ sample from the high mass-squared tail of the (π-K) signal. Our results have been corrected for all these effects.

The second group of counters, the Hadron Arm Time of Flight (HATOF) counters, is located 5.5 m from the interaction point and outside the coil (1.0 radiation lengths of Aluminium thick). The HATOF array in each arm consists of 48 separate scintillators (2.6 m high, 33 cm wide and 2 cm thick) equipped with photomultipliers at each end. Arranged in two rows of 24, one above the other, the counters form walls of scintillator in each arm 5.2 m high and approximately 8 m wide which together cover 20 % of the solid angle. The calibration and operation of the HATOF system will be described fully in a separate publication[6]. The rms timing resolution for tracks with momentum ~1 GeV/c is 0.5 nsec averaged over the counters allowing π-K separation up to 1.1 GeV/c and (π/K)-p separation up to 2.2 GeV/c. Towards low momentum, multiple scattering worsens the effective resolution by increasing the error on the calculation of the particle flight-path but this does not impair the particle separation ability. The energy loss and multiple scattering in the coil are large for protons and antiprotons of momentum less than 1 GeV/c and $K^\pm$ less than 0.5 GeV/c leading to large uncertainties in the absorption and other correction factors. However, these are just the regions covered by the ITOF where the uncertainties are much smaller. Therefore the HATOF is not used for these particles in these low momentum regions.

Fig. 1(b) shows the reconstructed mass squared as computed from particle momentum and time of flight using the HATOF counters for tracks with momentum (0.5 - 1.1) GeV/c. We define π, K and $p,\bar{p}$ in a similar way as with the ITOF counters. The background from electrons in the HATOF-identified pion data is small ($\lesssim 10$ % for $p < 0.5$ GeV/c and negligible for higher momenta) owing to the electrons showering in the magnet coil. Our $p,\bar{p}$ estimate comes from the number of events with large mass-squared as shown in the insert in Fig. 1(b).

The observed number of particles detected by the HATOF counters must be corrected for interactions in the magnet coil and for decay in flight. The combination of these two effects reduces the rates at the HATOF counters to typically 0.7 (0.3) of the original rates for $\pi^\pm$ ($K^\pm$) at 0.75 GeV/c. In addition, we require that the HATOF track assignment be unambiguous by demanding that only one track enters a given HATOF counter and that its neighbouring counters do not contain a hit. This leads to an extra factor of 0.54. Also, we require that the reconstructed vertical coordinate of the track along the counter as determined from the relative timing of the photomultiplier tubes is consistent with the position determined by extrapolating the track from the central detector (an average correction factor of 0.8, the loss arising from multiple scattering in the coil at low momentum) and that the track passes the cuts imposed for the central detector[5] (factor 0.95).

The sizes of the data samples from the ITOF and HATOF used for this analysis are shown in Table 1. We have used tighter track cuts than those of reference 5 ($d < 2.5$ cm and $|z| < 10$ cm where d is the distance of closest approach to the origin in the (x,y) plane and z is the coordinate at the point of closest approach to the z axis (= beam direction)). This eliminates tracks coming from interactions of secondaries with the beam pipe. We have checked that our proton samples (and also our π and K samples) contain a negligible contribution from beam-gas interactions by studying events with production points 10-20 cm along the beam direction from the real interaction point. Also, all events containing proton candidates have been inspected to check that they do not have the distinctive one-hemisphere appearance of a beam-gas interaction. Our final sample contains equal numbers of p and $\bar{p}$.

Figs. 2(a) and (b) show the differential cross sections as a function of momentum for pions, kaons and protons plus antiprotons for the 12 and 30 GeV data respectively. The cross section normalization is determined from our previously published differential momentum spectra for all particles[3] and the size of the data samples available for the TOF counters. At each value of W there is an overall normalization uncertainty of 20 %. At momenta around

0.5 GeV/c the $\pi^\pm : K^\pm : p,\bar{p}$ yields are roughly in the ratio 30 : 5 : 1. However, as the particle momentum increases the yield of $K^\pm$ and $p,\bar{p}$ appears to grow with respect to that for $\pi^\pm$, as shown in Fig. 2(c).

The inclusive $(p,\bar{p})$ cross section integrated over the momentum range (0.5 - 2.2) GeV/c is 0.58 ± 0.19 (0.14 ± 0.04) nb at W = 12 (30) GeV not including the overall normalization uncertainties. Expressing these values as ratios to the muon pair cross section ($\sigma_{\mu\mu} = 4\pi\alpha^2/3s$ where $s = W^2$) gives $R_{p,\bar{p}} = \sigma(e^+e^- \to p,\bar{p}X)/\sigma_{\mu\mu} = 0.9 \pm 0.3$ (1.5 ± 0.4). Comparing this to the measured R values in this experiment[5], assuming neutron production to equal proton production and making the further assumption that no more than one baryon pair per event is produced, we estimate that at least 26 ± 9 (39 ± 11) % of e^+e^- annihilations to hadrons will produce baryon-antibaryon pairs.

In Figs. 3(a) and (b) we show our values for the scaling cross sections $(s/\beta)\, d\sigma/dx$ where $x = 2E/W$ for $\pi^\pm$, $K^\pm$ and $(p,\bar{p})$ for the 12 and 30 GeV data respectively. Fig. 3(c) compares our $\pi^\pm$ data to similar results at a centre of mass energy of 5.2 GeV[7] measured for x values larger than those from this experiment. While the data from the two experiments have approximately equal values of the scaling cross sections for $\pi^\pm$ at $x \sim 0.1$, the higher energy experiments at lower values of x have a steeper dependence on x than do the 5.2 GeV data for larger x values. This rise in the number of low-x particles with increasing centre of mass energy has been discussed previously[3].

We have compared our results on the fractions of $K^\pm$ produced in hadronic events as a function of momentum (Fig. 2(c)) to the predictions of a jet model with u,d,s,c,b quarks and gluon effects[8]. These predictions are insensitive to the hadronization transverse momentum parameter and the presence of gluon emission. Baryon production is not included. The model predicts the fraction of charged kaons to rise with momentum (eventually to ~0.3 at 4 GeV/c). Qualitatively this is also seen in the data.

To summarize, we have measured $\pi^\pm$, $K^\pm$ and $(p,\bar{p})$ production in e^+e^- annihilations at centre of mass energies of 12 and 30 GeV. The fractional yield of charged kaons and baryons appears to rise with outgoing momentum. The scaling cross section for $\pi^\pm$ is similar to that obtained at lower centre of mass energy. At 30 GeV we estimate that at least 40 % of events contain baryons.

Acknowledgements

We would like to thank the PETRA machine group for their tremendous efforts in making this experiment possible. We acknowledge the invaluable cooperation of all engineers and technicians at the collaborating institutions. In particular we are indebted to B.R. Diplock, J.A. Blisset and B.T. Payne (Rutherford Laboratory). The Wisconsin group wishes to thank the Physics Department and especially the High Energy Group and the Graduate School of Research of the University for support. Those of us from abroad wish to thank the DESY Directorate for the hospitality extended to us while working at DESY. One of us (P.K.) would like to thank the Alexander von Humboldt-Foundation for support through a Humboldt Award.

Table 1 The number of tracks identified as $\pi^\pm$, $K^\pm$ or $p,\bar{p}$ in the momentum ranges quoted and used in the analysis at W = 12 and 30 GeV.

	$\pi^\pm$	$K^\pm$	$p,\bar{p}$
ITOF	(0.3 < p < 0.6 GeV/c)	(0.4 < p < 0.6 GeV/c)	(0.5 < p < 1 GeV/c)
W=12 GeV	293	22	17
W=30 GeV	608	37	34
HATOF	(0.3 < p < 1.5 GeV/c)	(0.5 < p < 1.1 GeV/c)	(1 < p < 2.2 GeV/c)
W=12 GeV	52	10	2
W=30 GeV	206	14	13

REFERENCES

1. TASSO Collaboration, data reported by G. Wolf at EPS International Conference, Geneva 1979
2. JADE Collaboration, W. Bartel et al., Phys. Lett. 88B (1979) 171
3. TASSO Collaboration, R. Brandelik et al., Phys. Lett. 89B (1980) 418
4. TASSO Collaboration, R. Brandelik et al., Phys. Lett. 83B (1979) 261
5. TASSO Collaboration, R. Brandelik et al., Z. Physik C, 4, 87 (1980)
6. K.W. Bell et al., to be published
7. DASP Collaboration, R. Brandelik et al., Nucl. Phys. B148 (1979) 189
8. P. Hoyer et al., Nucl. Phys. B161 (1979) 349; The hadron fragmentation was treated as suggested by R.D. Field, R.P. Feynmann, Nucl. Phys. B136 (1978) 1.

Figure Captions

Fig. 1(a) Reconstructed mass squared for tracks with $0.4 < p < 0.6$ GeV/c for W = 30 GeV using information from the ITOF counters. The curve is a Monte Carlo prediction from the momentum spectra of Fig. 2(b). The insert is for $0.5 < p < 1.0$ GeV/c and includes an ITOF Monte Carlo prediction for the π/K spectrum from the HATOF results of Fig. 2(b).

(b) Reconstructed mass squared for tracks with $0.5 < p < 1.1$ GeV/c for W = 30 GeV using information from the HATOF counters. The curve is a Monte Carlo prediction from the momentum spectra of Fig. 2(b). The insert is for $1.0 < p < 2.2$ GeV/c and includes a prediction for the π/K spectrum from reference 8. Also shown is the $p,\bar{p}$ resolution normalized to our estimated number of $p,\bar{p}$.

Fig. 2(a) Differential momentum spectrum for $\pi^{\pm}$, $K^{\pm}$ and $(p,\bar{p})$ for W = 12 GeV.

(b) Differential momentum spectrum for $\pi^{\pm}$, $K^{\pm}$ and $(p,\bar{p})$ for W = 30 GeV.

(c) Fractions of $\pi^{\pm}$, $K^{\pm}$ and $p,\bar{p}$ of all charged hadrons as a function of particle momentum at 12 and 30 GeV. The curves are the predictions of a $q\bar{q}g$ model described in the text for the fraction of $K^{\pm}$ at W = 12 GeV (dotted line) and 30 GeV (solid line).

Fig. 3(a) Scaling cross section $(s/\beta)\, d\sigma/dx$ for $\pi^{\pm}$, $K^{\pm}$ and $(p,\bar{p})$ at W = 12 GeV.

(b) Scaling cross section $(s/\beta)\, d\sigma/dx$ for $\pi^{\pm}$, $K^{\pm}$ and $(p,\bar{p})$ at W = 30 GeV.

(c) Comparison of scaling cross sections for $\pi^{\pm}$ at W = 12 and 30 GeV with data at 5.2 GeV.

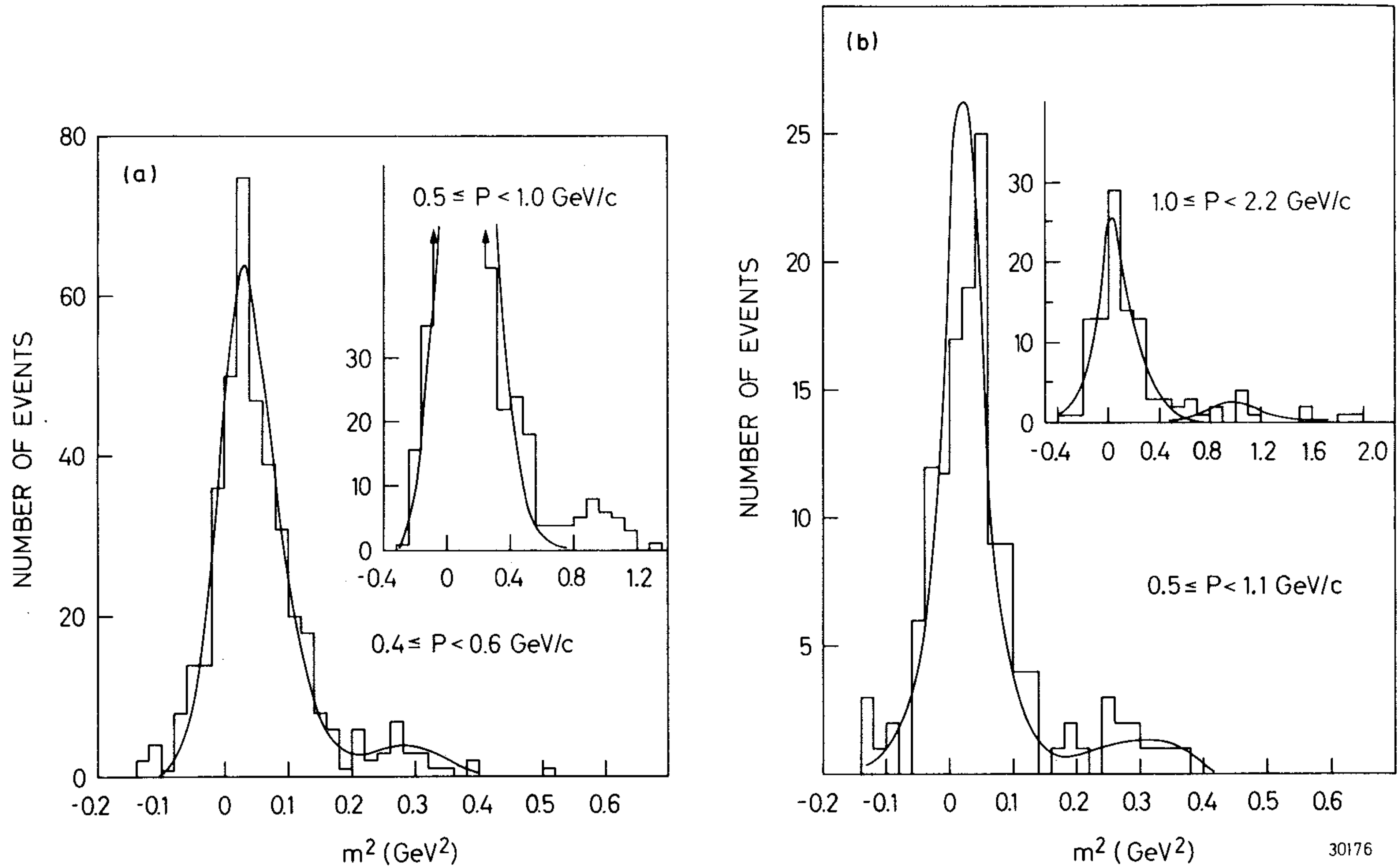
(a)
NUMBER OF EVENTS
0.5 ≤ P < 1.0 GeV/c
0.4 ≤ P < 0.6 GeV/c
m2 (GeV2)
(b)
NUMBER OF EVENTS
1.0 ≤ P < 2.2 GeV/c
0.5 ≤ P < 1.1 GeV/c
m2 (GeV2)
30176

Fig. 1

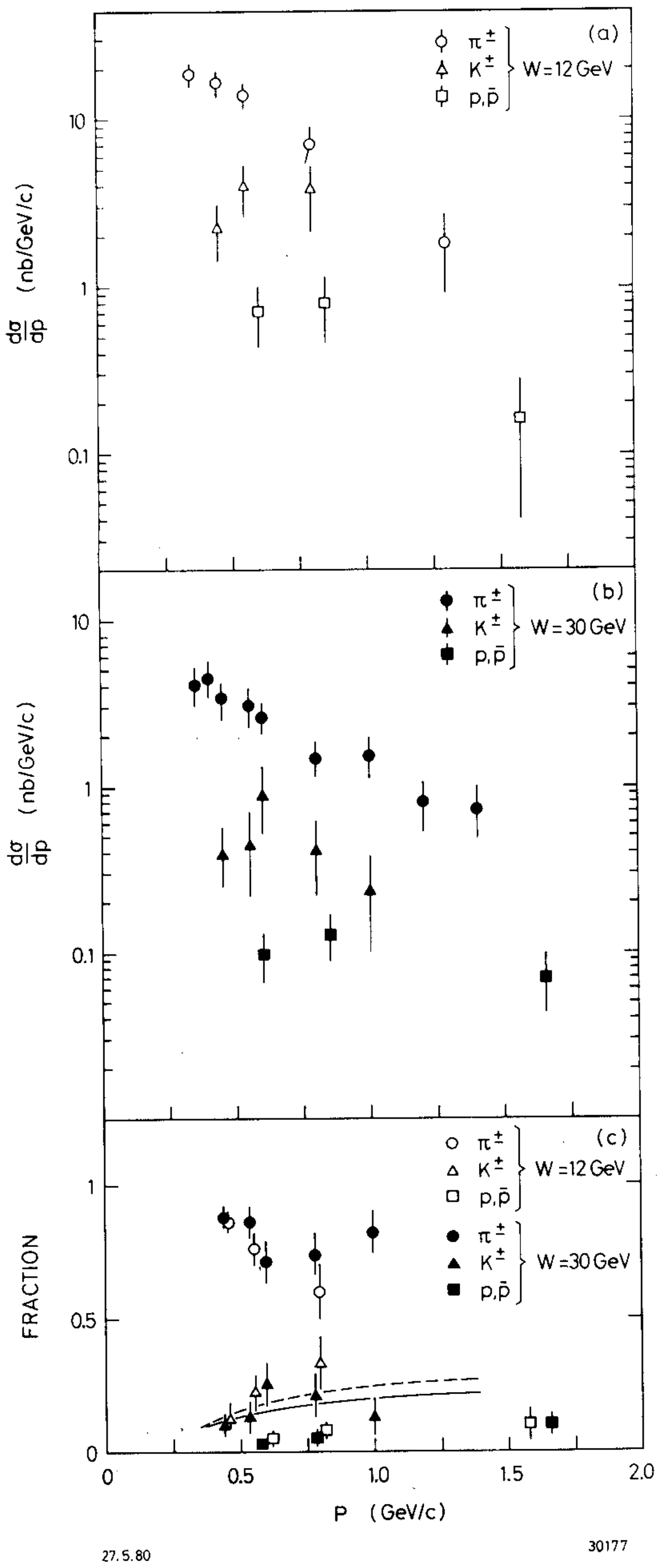

(a)
π±
K±
p,p̄
W=12 GeV
dσ/dp (nb/GeV/c)
10
1
0.1
(b)
π±
K±
p,p̄
W=30 GeV
(c)
W=12 GeV
W=30 GeV
FRACTION
0.5
0
1.0
1.5
2.0
P (GeV/c)
27.5.80
30177

Fig. 2

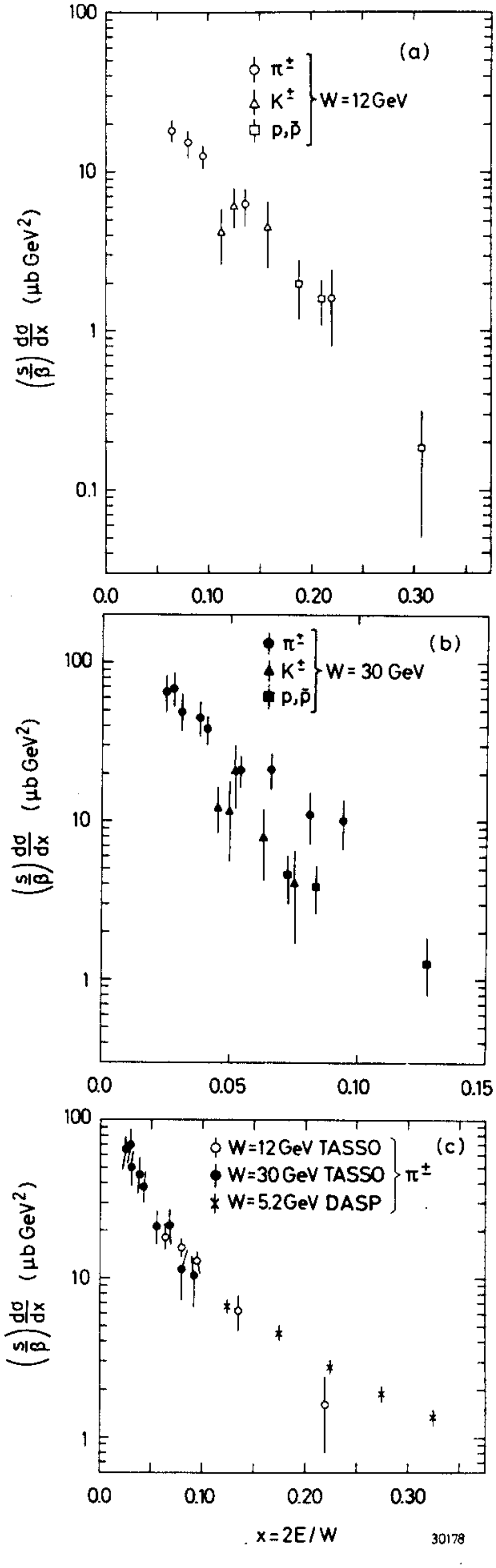

(a)
π±
K±
p, p̄
W = 12 GeV
(s/β) dσ/dx (μb GeV²)
(b)
π±
K±
p, p̄
W = 30 GeV
(c)
W=12 GeV TASSO
W=30 GeV TASSO
W=5.2 GeV DASP
π±
x = 2E/W
30178

Fig. 3